Biomaterials Science

ROYAL SOCIETY OF CHEMISTRY

PAPER

View Article Online
View Journal | View Issue

Cite this: *Biomater. Sci.*, 2023, **11**, 6790

Efficient fabrication of thermo-stable dissolving microneedle arrays for intradermal delivery of influenza whole inactivated virus vaccine

Jihui Lee,[a] Martin Beukema,[b] Oliwia A. Zaplatynska,[a] Conor O'Mahony,[c] Wouter L. J. Hinrichs,[d] Anke L. W. Huckriede,[b] Joke A. Bouwstra[a] and Koen van der Maaden *[a,e]

Dissolving microneedle arrays (dMNAs) can be used to deliver vaccines *via* the intradermal route. Fabrication of dMNAs using centrifugation is the most common preparation method of dMNAs, but it results in a substantial loss of antigens. In order to solve the issue of antigen waste, we engineered an automatic dispensing system for dMNA preparation. Here, we report on the fabrication of influenza whole inactivated virus (WIV) vaccine-loaded dMNAs (WIV dMNAs) by using the automatic dispensing system. Prior to the dispensing process, polydimethylsiloxane (PDMS) moulds were treated with oxygen plasma to increase surface hydrophilicity. WIV dMNAs were prepared with 1% (w/v) trehalose and pullulan (50 : 50 weight ratio). During the dispensing process, reduced pressure was applied to the PDMS mould *via* a vacuum chamber to make microneedle cavities airless. After producing dMNAs, WIV was quantified and 1.9 μg of WIV was loaded per dMNA, of which 1.3 μg was in the microneedle tips. Compared to the centrifugation method, this automatic dispensing system resulted in a 95% reduction of antigen waste. A hemagglutination assay confirmed that WIV dMNA maintained the stability of the antigen for at least four weeks of storage, even at room temperature or at 37 °C. The WIV dMNAs displayed 100% penetration efficiency in human skin, and 83% of the microneedle volume was dissolved in the skin within 10 minutes. In a vaccination study, mice immunised with WIV dMNAs showed similar IgG levels to those that received WIV intramuscularly. In conclusion, using the automatic dispensing system for dMNA production strongly reduced antigen waste and yielded dMNAs with excellent physical, mechanical, and immunological properties.

Received 2nd March 2023,
Accepted 10th August 2023

DOI: 10.1039/d3bm00377a

rsc.li/biomaterials-science

1. Introduction

Influenza viruses cause respiratory infections accompanied by symptoms, such as cough, fever, and sore throat. Influenza can be life-threatening, especially for older adults or people who have a weakened immune system.[1,2] Annually 3–5 million cases of severe illness and 290–650 thousand deaths are reported worldwide.[2] Fortunately, vaccines are available to control the infection. For example, the influenza vaccine decreased the illness rate in children by three times and the mortality rate in the elderly by 47%.[3,4] Most influenza vaccines are injected as an aqueous suspension using hypodermic needles. One of the major drawbacks of aqueous dosage forms is thermal instability. They require a cold chain to maintain antigen integrity and functionality. Another disadvantage of injectables is needle phobia. People who are afraid of needles hesitate to get their vaccination. According to a recent review, approximately 16% of adult people didn't get the influenza vaccine because of needle fear.[5] In order to solve these issues and increase the vaccination coverage rate, novel vaccine delivery methods are required.

Dissolving microneedle arrays (dMNAs), which have been introduced as novel vaccine delivery devices, can compensate for shortcomings of delivery *via* hypodermic needles. dMNAs are generally produced by vacuum filling or centrifugation.[5,6] After dermal application, they dissolve in the skin, thereby releasing encapsulated antigens. Sequentially, the antigens reach antigen presenting cells that are present in the viable

[a]*Division of Biotherapeutics, Leiden Academic Centre for Drug Research, Leiden University, 2333CC Leiden, The Netherlands*
[b]*Department of Medical Microbiology and Infection Prevention, University of Groningen, University Medical Center Groningen, 9713AV Groningen, The Netherlands*
[c]*Tyndall National Institute, Lee Maltings, Prospect Row, Cork, Ireland*
[d]*Department of Pharmaceutical Technology and Biopharmacy, University of Groningen, 9713AV Groningen, The Netherlands*
[e]*Department of Immunology, Leiden University Medical Center, 2300RC Leiden, The Netherlands*

epidermis and dermis of the skin. Several advantages of dMNAs are identified. Because of their short length, dMNAs can reduce pain sensation during administration.[7,8] As the microneedle tip dissolves in the skin during the application, they also avoid sharps waste. Besides, dMNAs allow self-administration without trained medical staff.[9]

The solid dosage form of dMNAs can maintain the thermal stability of antigens, allowing cost-effective vaccine delivery as a cold chain can be avoidable. Maintaining antigen stability and antigenicity is crucial and can be fulfilled by optimising the dMNA formulation. In various studies, it has been shown that several influenza antigens in dMNAs were stable at 25 °C for the long term (over 28 days, 81 days, and 24 months).[10–12] Plasmid DNA encoding a green fluorescent protein (GFP-pDNA) in polylactide dMNAs also proved its stability by inducing a similar protein expression to naked GFP-pDNA from stock solution after storage at 45 °C for 60 days.[13]

Despite many benefits, the drawback of most dMNA fabrication methods is the huge waste of antigens during fabrication. For example, dMNAs fabricated with a centrifugation method carry more antigens in the backplate than in the microneedle tips. As only these tips are pierced into the skin, a substantial amount of antigen gets lost. In our previous study, we produced influenza whole inactivated virus (WIV) loaded dMNAs (WIV dMNAs) using the centrifugation method and proved that they were able to induce high levels of protective antibody responses.[12] However, the delivery efficiency of these dMNAs was very low, *i.e.* 12.5 μg of WIV was loaded in a single dMNA to deliver 1 μg (92% antigen loss). Therefore, optimisation of the fabrication method is required to reduce antigen waste and decrease production costs.

In order to reduce antigen waste, production methods for dMNAs have been developed that localise antigens primarily in the microneedle tips. Filling polydimethylsiloxane (PDMS) moulds, which is a porous container, with a sprayed formulation[14] or dispensed droplets[15,16] resulted in lower drug waste in the backplate. In our previous work, we reported an automatic dispensing system as a drug-saving fabrication method for dMNAs by loading the drug only in the microneedle tips and proved a reduction in drug waste of 98.5%.[17]

The aim of this study was to evaluate the applicability of our previously developed nano-dispensing system for antigen-efficient fabrication of dMNAs.[17] In this study, we developed WIV dMNAs with reduced antigen loss, aiming to induce protective immune responses. First, trehalose/pullulan dMNAs were fabricated by using the automatic dispensing system. For this, the concentration of trehalose/pullulan was optimised for both empty dMNAs (without WIV) and WIV dMNAs. Next, the stability of WIV in WIV dMNAs was investigated after four weeks of storage under three different conditions (4 °C, room temperature (RT), and 37 °C with 0% relative humidity (RH)). WIV loading was quantified to examine the repeatability of the fabrication method. Finally, WIV was administered in mice through WIV dMNAs and intramuscular (I.M.) injection, and the immune responses were compared.

2. Materials and methods

2.1. Materials

Silicon microneedle arrays were obtained from Tyndall National Institute (Cork, Ireland). SYLGARD 184 base silicone elastomer and curing agent silicone elastomer were purchased from Dow Corning (Midland, MI, USA). Pullulan (average molecular weight 200–300 kDa) and trehalose were kindly provided by Hayashibara Co., Ltd (Okayama, Japan). Trypan blue solution 0.4% (w/v) was purchased from Millipore Sigma (Zwijndrecht, The Netherlands). Vinylpolysiloxane A-silicone (Elite Double 32) was purchased from the Zhermack Group (Badia Polesine, Italy) and epoxy glue was obtained from Bison International B.V. (Goes, The Netherlands). Tape (packing tape, polypropylene, transparent) for stripping skin was purchased from Staples (Almere, Netherlands) and guinea pig red blood cells were obtained from Envigo (Horst, The Netherlands). 4-(2-Hydroxyethyl)-1-piperazineethanesulfonic acid (HEPES)-buffer and micro BCA protein assay kits were purchased from Thermo Fisher Scientific (Bleiswijk, Netherlands).

2.2. Preparation of influenza whole inactivated virus vaccine

NIBRG-121 (National Institute of Biological Standards and Controls, Potters Bar, United Kingdom), a reassortant carrying the hemagglutinin of A/California/7/2009 H1N1pdm09 influenza virus, was used to prepare WIV as previously described.[12] In short, the virus was propagated in the allantoic cavity of 11-day-old hen's eggs. After 72 hours of incubation at 37 °C, the virus was isolated and purified from the allantoic fluid. The virus was inactivated with β-propiolactone (0.1% v/v) by overnight incubation under continuous rotation at 4 °C. Next, WIV was dialysed against HEPES-buffered saline at 4 °C overnight to remove β-propiolactone. Inactivation of the virus was verified by inoculating Madin–Darby Canine Kidney (MDCK) cells and assessed with a hemagglutination assay as previously described.[18] The total protein concentration of WIV was determined with the micro-Lowry assay.[19]

2.3. Preparation of PDMS moulds

As previously described, the polymethylmethacrylate (PMMA) grid was made by the Fine Mechanical Department at Leiden University.[17] This grid consisted of nine (3 × 3) pedestals, and a silicon microneedle array was attached with glue on each pedestal of the grid. The silicon microneedle array had nine (3 × 3) microneedles with a height of 500 μm and a base diameter of 330 μm. The combination of the grid and silicon microneedle arrays was a master structure. From this master structure, a PDMS mould was prepared.[20] Briefly, a Sylgard 184 base silicone elastomer and a curing agent were mixed at a 10 : 1 weight ratio, and around 20 g of this mixture was poured into the master structure. After the mixture was cured overnight at 60 °C, the cured PDMS mould was carefully detached from the master structure. A successfully fabricated PDMS mould should contain nine negative arrays (3 × 3 arrangement), and

each array should consist of nine microneedle cavities (3 × 3). Therefore, one mould had in total 81 microneedles.

2.4. Oxygen plasma treatment of the PDMS mould

An intact microneedle should have a sharp conical tip, which can be created when there is no air gap between the microneedle cavity of PDMS mould and the aqueous dMNA formulation. To remove this gap by increasing the hydrophilicity of the PDMS surface, oxygen plasma treatment was applied. The hydrophilic surface increases the wettability and interaction between the PDMS surface and the formulation.

The surface modification of the PDMS mould was performed in a plasma chamber (Femto model 1A, Diener Electronic, Ebhausen, Germany). The oxidation power (10–50 W) and exposure period (10–120 seconds) were varied, while the system pressure and the flow rate of oxygen were kept constant at 100 μbar and 25 sccm, respectively. In order to select the most effective oxidation conditions of the oxygen plasma treatment, the epoxy glue was applied on the plasma-treated PDMS mould and dried at 37 °C. After 2 hours, it was attempted to remove the glue from the mould. The highest oxidation conditions that resulted in the successful removal of the glue from the mould without breaking the mould were selected for further studies.

2.5. Screening of trehalose and pullulan concentration

In our previous study, we used a centrifugation method for the dMNA fabrication, and 15% (w/v) trehalose/pullulan in phosphate buffer (PB, pH 7.4, prepared with 7.7 mM Na_2HPO_4 and 2.3 mM NaH_2PO_4) was used for the dMNA formulation.[12] Compared to the centrifugation method, the viscosity of dMNA formulations is a critical factor for the automatic dispensing system because too high viscosity of the formulation does not produce droplets. In order to find the most suitable formulation, the concentration of trehalose/pullulan was varied from 1% (w/v) to 15% (w/v) with a trehalose : pullulan weight ratio of 50 : 50. Next, the formulation was loaded into the dispenser (PipeJet® Nanodispenser, BioFluidix GmbH, Germany) and it was tested whether droplets were successfully formed or not. Only formulations that resulted in droplets were selected for further studies.

2.6. Fabrication of the empty dMNA

In order to penetrate the skin and successively release their content, sharp and strong microneedles are required. To investigate whether the selected formulations (section 2.5) were suitable to fabricate sharp and strong microneedles, first, empty dMNAs were fabricated as previously described.[17]

Briefly, the selected formulations were loaded into the dispenser. Then, the PDMS mould was placed on the vacuum chamber, which was installed on the *z*-stage (Physik Instrumente Benelux B.V., The Netherlands). Vacuum was required to remove air bubbles that were potentially trapped in microneedle cavities of the mould. To completely fill the microneedle cavity, 20 dispensing cycles were required.

2.6.1 One cycle. The nozzle of the dispenser and the first microneedle cavity in the mould were aligned, and one droplet (around 14 nL) was shot into the microneedle cavity. Next, *x*- and *y*-stages moved and aligned the nozzle with the next microneedle cavity to fill it with another droplet. This alignment of the microneedle cavity with the nozzle and dispensing of droplets were repeated until the last microneedle cavity in the mould was filled.

After all 81 microneedle cavities were completely filled, the mould was placed at 37 °C to solidify the formulation. The leftover formulation in the nozzle and the tube was re-collected to minimise the antigen waste. The next day, epoxy glue was applied over the microneedle cavities to form a backplate, and subsequently dried at 37 °C. After 2 hours of drying, empty dMNAs were carefully removed from the mould.

The appearance of microneedles was analysed using a brightfield microscope (Stemi 2000-C, Carl Zeiss Microscopy GmbH, Göttingen, Germany), and the number of intact microneedles was determined. The most suitable formulation (5% (w/v) trehalose/pullulan, see section 3.2), which resulted in the highest percentage of intact microneedles, was selected for further studies.

2.7. Skin penetration and dissolution tests

The ability to penetrate the skin is an essential function of dMNAs for successful vaccine delivery. For this evaluation, a skin penetration test was performed.[21] Human abdominal skin was obtained from a local hospital, and excess fat was removed from the skin. After stretching the skin on parafilm-covered Styrofoam, the surface of the skin was wiped with 70% (w/v) ethanol. Next, the dMNA was attached to the applicator (uPATCH B.V., Delft, The Netherlands). The dMNA was inserted into the skin with a constant velocity (65 ± 1 cm s^{-1}) and automatically removed after one second. Then, 75 μL of a trypan blue solution (0.4%) was applied on the microneedle-treated skin site. After 45 minutes, the excess of trypan blue was removed, and subsequently the stratum corneum was removed by tape-stripping until the skin became shiny. The dMNA-treated skin site was analysed using a brightfield microscope and the penetration efficiency was calculated by dividing the number of blue dots on the skin by the number of total microneedles in one dMNA (nine microneedles/array). The penetration studies were done in triplicate.

A skin dissolution test was carried out to find the dissolution time and the dissolved volume of microneedles, preferably over 70% of the microneedle volume should be dissolved within 30 minutes for the convenience of the administration. The dMNA was applied on the skin in the same manner as that explained for the skin penetration test in this section. However, the microneedles stayed in the skin for prolonged periods (15 and 30 minutes) before withdrawal in order to test the dissolution properties. The shape and height of the leftover microneedles after withdrawal were analysed using the brightfield microscope. Based on the leftover height of the microneedle, its dissolved volume was calculated.

2.8. Fabrication of WIV dMNAs

As the addition of WIV might change the viscosity of the trehalose/pullulan formulation, the formulation for WIV dMNAs was further optimised. To this end, the selected concentration of the trehalose/pullulan mixture (5% (w/v), see section 3.2) was reduced to 3, 2, and 1% (w/v). To these reduced trehalose/pullulan concentrations, WIV was added to obtain a final concentration of 0.75 mg mL^{-1} (stock concentration: 2.8 mg mL^{-1}). The WIV dMNA was fabricated as described in section 2.6. Among three formulations, the formulation that did not clog the nozzle was selected. Fabricated WIV dMNAs were imaged using the brightfield microscope, and the number of intact microneedles was counted. Finally, skin penetration and dissolution tests were performed as described in section 2.7, and the penetration efficiency and dissolution ability were assessed.

2.9. Quantification of WIV loading in WIV dMNAs

The amount of WIV in WIV dMNAs was quantified to determine whether sufficient WIV can be delivered into the skin to effectively provoke immune responses. Based on the concentration of WIV and the dispensed volume of formulation, approximately 1.9 μg of WIV was expected to be loaded in each WIV dMNA: 14 nL droplet; 0.75 mg mL^{-1} WIV; 9 microneedles in one dMNA;20 dispensing cycles. In order to examine the actual loading amount of WIV in each part of the dMNA, both (1) the whole WIV dMNA and (2) the backplate groups were prepared (Fig. 1, $n = 3$). The backplate group was prepared by removing nine microneedles from the whole WIV dMNA. The amount of WIV in nine microneedles was calculated by subtracting the WIV amount in the backplate (group 2) from the amount in the whole WIV dMNA (group 1).

The amount of WIV in both groups was quantified by a bicinchoninic acid (BCA) assay. For the BCA assay, both the whole WIV dMNA and backplate were reconstituted in 350 μL of PB and homogenised overnight. Then, 100 μL of the homogenised solution was loaded into a 96-well plate. For the calibration curve, 0.07 μg μL^{-1} WIV in 1% (w/v) trehalose/pullulan was prepared and two-fold serial dilutions were obtained. Next, 150 μL of the working reagent was added. After 2 hours of incubation at 37 °C, the absorbance was measured at 562 nm using a Tecan Infinite M1000 plate reader (Männedorf, Switzerland).

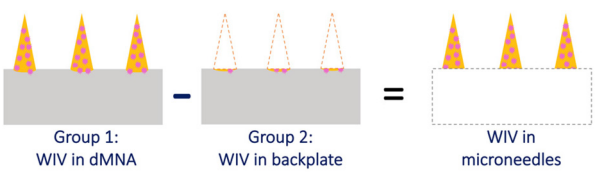

Fig. 1 WIV amount in each part of the dMNA. Dispensed droplets slightly filled over the microneedle cavity. Therefore, there is some WIV and trehalose/pullulan formulation in the backplate after the removal of microneedles.

2.10. Stability of WIV in WIV dMNAs

It is crucial to secure long term antigen integrity and stability to provoke protective immune responses upon administration of dMNAs. Therefore, stability and activity of WIV in WIV dMNA were examined after four weeks of storage, as we learned from previous studies that non-refrigerated WIV in aqueous formulations become completely dysfunctional after four weeks of storage.[12] First, WIV dMNAs ($n = 3$) and WIV dispersed in PB ($n = 3$) were stored under three different conditions: 4 °C/0% RH, RT/0% RH, and 37 °C/0% RH. The functionality of WIV in both WIV dMNAs and WIV dispersion was tested by a hemagglutination assay. After storage, WIV dMNAs were reconstituted in PB. Then, ten series of two-fold dilutions of PB with dissolved WIV dMNAs, WIV dispersion, and freshly prepared WIV dispersion (positive control group) were placed in a 96-well plate. Next, 50 μl of 1.5% (v/v) guinea pig red blood cell suspension were added into the wells and incubated for 1.5 hours at RT. Lastly, the hemagglutination titer was determined by reading the agglutination of red blood cells.

2.11. Immunisation of mice with dMNAs and sample collection

The Central Committee for Animal Experimentation of the Netherlands approved the animal procedures of this study (CCD application number AVD105002016599). Female CB6F1 (C57Bl/6 x BALB/c F1) mice of 6–8 weeks were acclimatised for 1.5 weeks before the start of the experiment. Mice were co-housed with three mice in individually ventilated cages and had *ad libitum* access to sterilised tap water and a standard diet. Mice were vaccinated with WIV dMNAs as described below or received an I.M. injection in the right thigh with an aqueous WIV dispersion of 1 μg in 25 μl of PBS. As a negative control, empty dMNAs were applied on the ear pinnae. A total number of six mice per experimental group were used. The dMNAs were attached to the piston of a digitally-controlled microneedle applicator (Check v1.0, uPATCH B.V., Delft, The Netherlands) using double-sided tape. Next, the mice were anaesthetised with isoflurane and subsequently, the applicator was placed onto the right ear. The dMNAs were applied with a velocity of 65 ± 1 cm s^{-1} and kept in place for 10 minutes and then removed. At 28 days post-immunisation, mice were sacrificed. Blood was collected by heart puncture and clotted overnight at RT. Next, blood was centrifuged for 10 minutes at 3000 RCF and the serum was used for ELISA (see below). Spleens were collected in 2.5 ml of Iscove's modified Dulbecco's medium (IMDM; Thermo Fisher Scientific, Bleiswijk, Netherlands) containing 10% v/v FBS (Lonza, Basel, Switzerland), 100 U ml^{-1} penicillin, 100 mg ml^{-1} streptomycin and 50 μM 2-mercaptoethanol (Invitrogen, Breda, The Netherlands) and used for ELISPOT (see below).

2.12. ELISA

To determine total IgG, IgG1 or IgG2a levels in the serum, ELISA was performed as previously described.[21] For the detection of total IgG, A(H1N1)pdm09 WIV was used as coating. The

serum samples were diluted 1 : 200 and applied in a 2-fold serial dilution on the plates. The horseradish peroxidase (HRP)-linked goat anti-mouse IgG (Southern Biotech, Birmingham, USA) antibody was used to detect bound IgG. Total IgG titers were calculated as log 10 of the reciprocal of the serum sample dilution corresponding to an absorbance of 0.2 at a wavelength of 492 nm. To detect IgG1 and IgG2a levels, goat-anti mouse IgG antibody (Southern Biotech, Birmingham, USA) was used as a coating. Here, serum samples were applied in a dilution of 1 : 100 and HRP-linked goat anti-mouse IgG1 (Southern Biotech, Birmingham, USA) or HRP-linked goat anti-mouse IgG2a (Southern Biotech, Birmingham, USA) was used for detection. IgG1 and IgG2a concentrations were determined from a standard curve (Southern Biotech, Birmingham, USA). The IgG2a/IgG1 ratio was calculated by dividing the concentration of IgG2a by the concentration of IgG1 in each mouse.

2.13. ELISPOT

A mouse enzyme-linked immunosorbent spot (ELISPOT) kit (MABTEC, The Netherlands) was used according to the manufacturer's instructions to assess influenza-specific interferon (IFN)-γ and interleukin (IL)-4 secreting splenocytes. In short, spleens were homogenised using a gentleMACS Dissociator (Miltenyi Biotec, Leiden, The Netherlands). Then erythrocytes were lysed by washing them with ammonium–chloride–potassium lysis buffer (0.83% NH_4Cl, 10 mM $KHCO_3$, and 0.1 mM ethylenediaminetetraacetic acid (EDTA)). The splenocytes (5×10^5 per well) were incubated in IMDM complete medium (with 10% FBS, 1% penicillin–streptomycin and 0.1% β-mercaptoethanol) with or without 10 μg ml^{-1} A(H1N1) pdm09 WIV in wells precoated with the respective capture antibody. After 16 hours of incubation at 37 °C, IFN-γ or IL-4 secreting splenocytes were detected using alkaline phosphatase-linked anti-mouse IFN-γ or IL-4 antibodies,[22] respectively. Spots were developed using nitro-blue tetrazolium chloride/5-bromo-4-chloro-3′-indolyphosphate *p*-toluidine substrate and counted with an Autoimmune Diagnostika (AID GmbH, Strassberg, Germany) ELISPOT reader. The number of spots representing influenza-specific T cells was calculated by subtracting the number of spots in the untreated wells from the number of spots in the WIV-treated wells.

2.14. Statistics

Statistical analysis of results was performed using GraphPad Prism version 8.4.1 (La Jolla, CA, USA). Data was tested with the Kruskal–Wallis test and Dunn's *post hoc* test. $p < 0.05$ was considered as a significant difference; * $p < 0.05$, ** $p < 0.01$.

3. Results

3.1. Oxygen plasma treatment of PDMS moulds

To achieve intact and sharp microneedle tips, increasing the cohesion between the formulation and the surface of microneedle cavities is important. To make the PDMS surface more hydrophilic, oxygen plasma treatment was performed on the PDMS mould with various oxidation powers and exposure times. As shown in Table 1, the epoxy glue could be removed easily from the mould when the mould was treated with 10 W oxidation power for 5–60 seconds. Exposure of PDMS moulds to a higher power or longer period hindered the removal of the glue because of the too strong attraction between the mould and the glue. Among the four oxidation conditions that enabled the removal of the glue, 10 W and 60 seconds were selected as these conditions were the maximum oxidation conditions that allowed the strongest hydrophilicity of the mould while the glue could still be removed from the mould without destroying it.

Table 1 Affinity between the epoxy glue and PDMS moulds based on various oxidation conditions

Oxidation power (W)	Exposure period (s)	Results
50	10, 30, 60, 90, and 120	Glue was attached to the PDMS mould and could not be separated without destroying the mould
40		
30		
20		
17.5		
15		
10	120	
	90	
	60	Glue was removed without destroying the mould
	30	
	10	
	5	

3.2. Optimisation of trehalose and pullulan concentration for the empty dMNA formulation

The dispenser can only produce droplets with low viscosity formulations (<50 mPa s), thus, screening the dispensable formulations is required to fabricate the microneedle. Out of 15 initial formulations varying in the concentration of trehalose/pullulan from 1 to 15% (w/v), only formulations containing 1–5% (w/v) trehalose/pullulan droplets were obtained without clogging the dispenser.

There was no microneedle structure when using 1% (w/v) trehalose/pullulan as the trehalose/pullulan amount in each microneedle cavity was too low to build the microneedle structure. However, the usage of increased trehalose/pullulan concentrations (2–5% (w/v)) resulted in the formation of microneedles.

As shown in Fig. 2, the percentage of intact microneedles increased together with the concentration of trehalose/pullulan. When the concentration was increased from 2% to 3%, 4%, and 5% (w/v), the average percentage of intact microneedles increased from 32.5 ± 2% (Fig. 2a) to 50.2 ± 1% (Fig. 2b), 77.8 ± 1% (Fig. 2c), and 96.7 ± 1% (Fig. 2d), respectively (mean ± SD, $n = 3$). As 5% (w/v) trehalose/pullulan resulted in the highest rate of intact microneedles, the skin penetration and dissolution tests were performed with empty dMNAs prepared with this formulation.

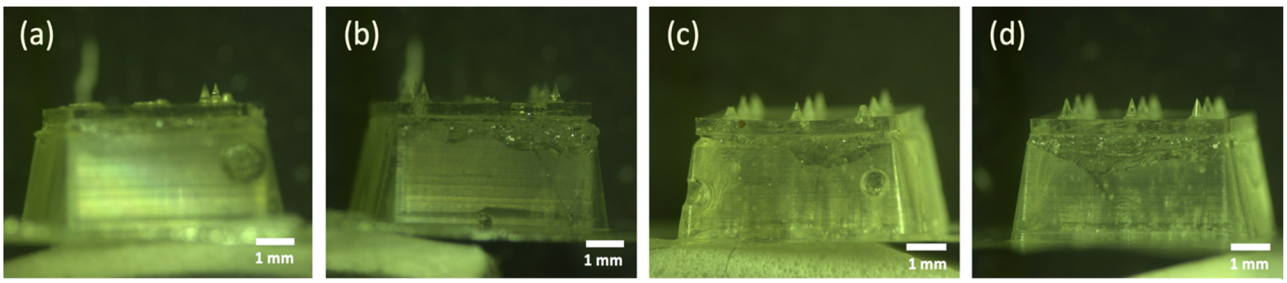

Fig. 2 Representative microscopic images of fabricated empty dMNAs using the automatic dispensing system. Empty dMNAs were produced with (a) 2% (w/v), (b) 3% (w/v), (c) 4% (w/v), and (d) 5% (w/v) trehalose/pullulan (n = 3). The weight ratio of trehalose to pullulan was 50 : 50.

3.3. Skin penetration and dissolution tests of empty dMNAs

The rigidity and dissolution rate are crucial characteristics of the dMNA for effective administration into the skin. Therefore, skin penetration and dissolution tests were essential to determine whether the empty dMNA prepared with 5% (w/v) trehalose/pullulan is suitable for vaccine delivery.

As shown in Fig. 3a, all nine microneedles penetrated the skin: 100% penetration efficiency (n = 3). After dissolution in the skin, the sharp microneedle tips (Fig. 3b) became blunt. The remaining height of the microneedles was 132.3 ± 0.3 (Fig. 3c) and 49.8 ± 2 (Fig. 3d) after 15 minutes and 30 minutes of dissolution, respectively.

3.4. Fabrication of dMNAs with WIV and skin penetration/dissolution tests

As 5% (w/v) trehalose/pullulan was selected for the formulation of empty dMNAs, 0.75 mg mL^{-1} WIV was loaded into this formulation and WIV dMNAs were produced and analysed as above. However, the addition of WIV to 5% (w/v) trehalose/pullulan increased the viscosity, so that the formulation was not dispensable through the nozzle. Therefore, the concentration of trehalose/pullulan was reduced to 1, 2 and 3% (w/v). When containing WIV, the nozzle clogged with 3% and 2% trehalose/pullulan while 1% trehalose/pullulan was well dispensable without clogging the nozzle. Therefore, 1% (w/v) trehalose/pullulan was selected to formulate the WIV dMNA. With the oxygen plasma-treated PDMS mould, WIV dMNAs showed 98.4 ± 1% (n = 3) of intact microneedles (Fig. 4a).

Similar to empty dMNAs, the mechanical strength and dissolution ability of WIV dMNAs were assessed by skin penetration and dissolution tests. The penetration efficiency of WIV dMNAs was similar to that of empty dMNAs as again 100% of penetration efficiency was obtained. The remaining height of the microneedles was 105.8 ± 3 (Fig. 4b), 57.3 ± 2 (Fig. 4c), and

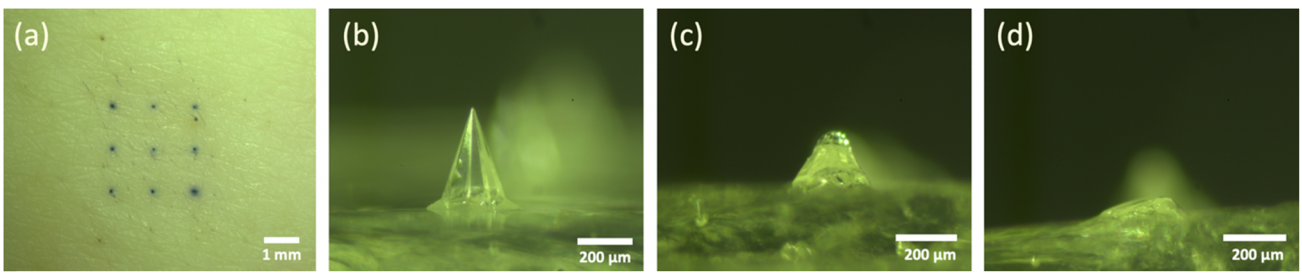

Fig. 3 Representative microscopic images of skin penetration and dissolution tests of empty dMNAs (n = 3). (a) Human abdominal skin *ex vivo* penetrated with a 5% (w/v) trehalose/pullulan 3 × 3 dMNA. (b)–(d) Microneedle made of 5% (w/v) trehalose/pullulan (b) before skin dissolution and leftover microneedle (c) after 15 minutes and (d) after 30 minutes of skin dissolution.

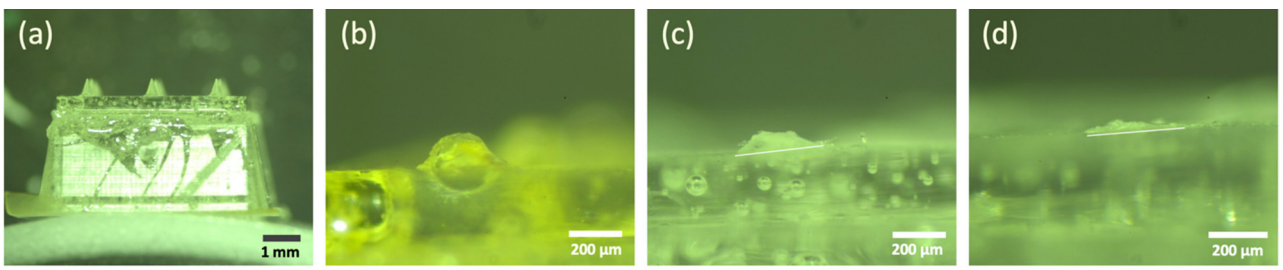

Fig. 4 (a) The fabricated WIV dMNA with 100% of intact microneedles. WIV loaded microneedles after (b) 2 minutes, (c) 5 minutes, and (d) 10 minutes of skin dissolution. The shape of the intact microneedle before dissolution was similar to that in Fig. 3b. Longer dissolution times were not evaluated as the leftover volume after 10 minutes was sufficiently low.

28.1 ± 2 (Fig. 4d) after 2, 5, and 10 minutes of dissolution, respectively.

3.5. Quantification of the amount of WIV in the WIV dMNA

Knowing the WIV loading amount in the microneedle tips is important to determine the maximum delivered dose into the skin. Therefore, the loaded amount of WIV in both the whole WIV dMNA and the backplate of the WIV dMNA was examined by a BCA assay. The BCA assay revealed that 1.9 ± 0.03 μg of WIV was loaded in the whole WIV dMNA while the backplate contained 0.6 ± 0.02 μg of WIV. By subtracting the WIV amount in the backplate from the WIV amount in the whole WIV dMNA, it was calculated that 1.3 μg of WIV was loaded in the nine microneedles.

As 84.1 ± 1% of the microneedle volume dissolved after 10 minutes of dissolution in the skin (see section 3.4), 1.1 ± 0.01 μg of WIV could theoretically be delivered into the skin. Therefore, the WIV dMNA carried a sufficient amount of WIV to deliver the target dose of 1 μg.

3.6. Stability of WIV in the WIV dMNA

By securing the stability of antigens, dMNAs could deliver the antigen and induce sufficient immune responses. In order to examine the stability of WIV, WIV dMNAs were stored for four weeks at 4 °C/0% RH, RT/0% RH, and 37 °C/0% RH, and a hemagglutination assay was performed to determine the activity of WIV.

As shown in Fig. 5, the functionality of WIV retrieved from WIV dMNAs dissolved in PB after storage was similar to that of fresh WIV dispersion under all three storage conditions (no significant difference). In contrast, the stored WIV dispersion showed a significant loss ($p < 0.01$) of WIV functionality compared to the control group (fresh WIV dispersion) under all three storage conditions. These results demonstrated that the incorporation of WIV in trehalose/pullulan dMNAs enhanced its stability as compared to WIV dispersion.

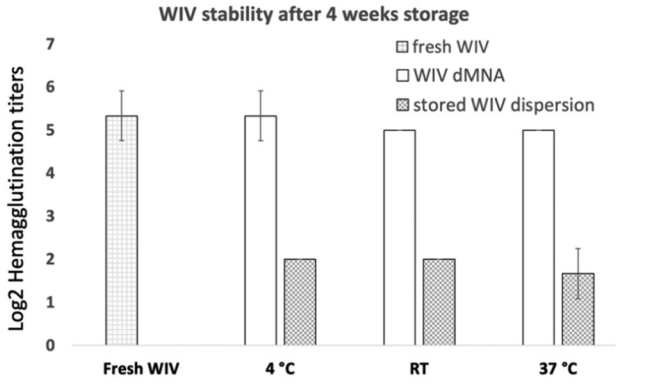

Fig. 5 WIV stability after four weeks of storage. The functionality of WIV in WIV dMNAs (white) and in WIV dispersion (dark grey) after four weeks of storage (n = 3) under different conditions. Fresh WIV which was not stored was used as the positive control (light grey). Results are represented as mean ± SD, n = 3; no error bars indicate that the SD was 0. As the log 2 value of hemagglutination titers came as an integer, SD can be 0 when the value is 2, 2, and 2.

3.7. Humoral and cellular immune responses evoked by immunisation with dMNA

Next, we investigated the capacity of WIV dMNAs to induce influenza virus-specific immune responses in mice, using responses elicited by traditional injection as a benchmark. Since the WIV dMNAs were able to deliver an amount of 1 μg of WIV into the skin, mice from the positive control group were I.M. injected with an aqueous formulation containing 1 μg of WIV. As a negative control, empty dMNAs were applied.

The evoked humoral immune responses were assessed by measuring the total influenza-specific IgG titer, IgG1 levels, and IgG2a levels in the serum of mice at 28 days post immunisation (Fig. 6). As shown in Fig. 6A, immunisation with WIV dMNAs induced similar levels of virus-specific IgG as immunisation *via* conventional I.M. injection. Quantification of IgG1 (Fig. 6B) and IgG2a (Fig. 6C) levels revealed that administration of WIV *via* both intradermal administration using the WIV dMNA and I.M. immunisation elicited both IgG subtypes. The resulting average IgG2a/IgG1 ratio was 1.98 for WIV dMNA immunisation and 3.53 for I.M. immunisation pointing to the induction of a balanced and a Th1-dominated antibody response for intradermal WIV dMNA and I.M. immunisation, respectively.[20]

The evoked cellular immune responses in mice were determined by measuring the levels of IFN-γ (Fig. 6E) and IL-4 (Fig. 6F) secreting splenocytes. Mice immunised with the WIV dMNA and I.M. injection both showed an increased level of IFN-γ secreting splenocytes, whereas they did not show an increased level of IL-4 secreting splenocytes. The number of IFN-γ secreting splenocytes was higher in I.M. injected mice than that in WIV dMNA-treated mice, confirming that I.M. injection of WIV might induce a stronger Th1 type cellular immune response than administration *via* WIV dMNAs.[23]

Taken together, the data demonstrate that immunisation with the WIV dMNA evokes comparable levels of immune responses as immunisation *via* I.M. injection but results in a somewhat less Th1-biased response.

4. Discussion

In this study, we explored a novel method for the fabrication of dMNAs and characterised the *in vitro* and *in vivo* properties of the produced dMNAs. In our previous work, the centrifugation method for WIV dMNA production resulted in a huge antigen loss (92% per dMNA) caused by focused antigen loading in the backplate.[12] By using the automatic dispensing system, WIV dMNAs were successfully engineered with minimal waste of antigens. In addition, these WIV dMNAs provoked immune responses of comparable magnitude as I.M. injected WIV. Therefore, the automatic nano-dispensing system used here brought many advantages over conventional techniques for dMNA fabrication as explained below.

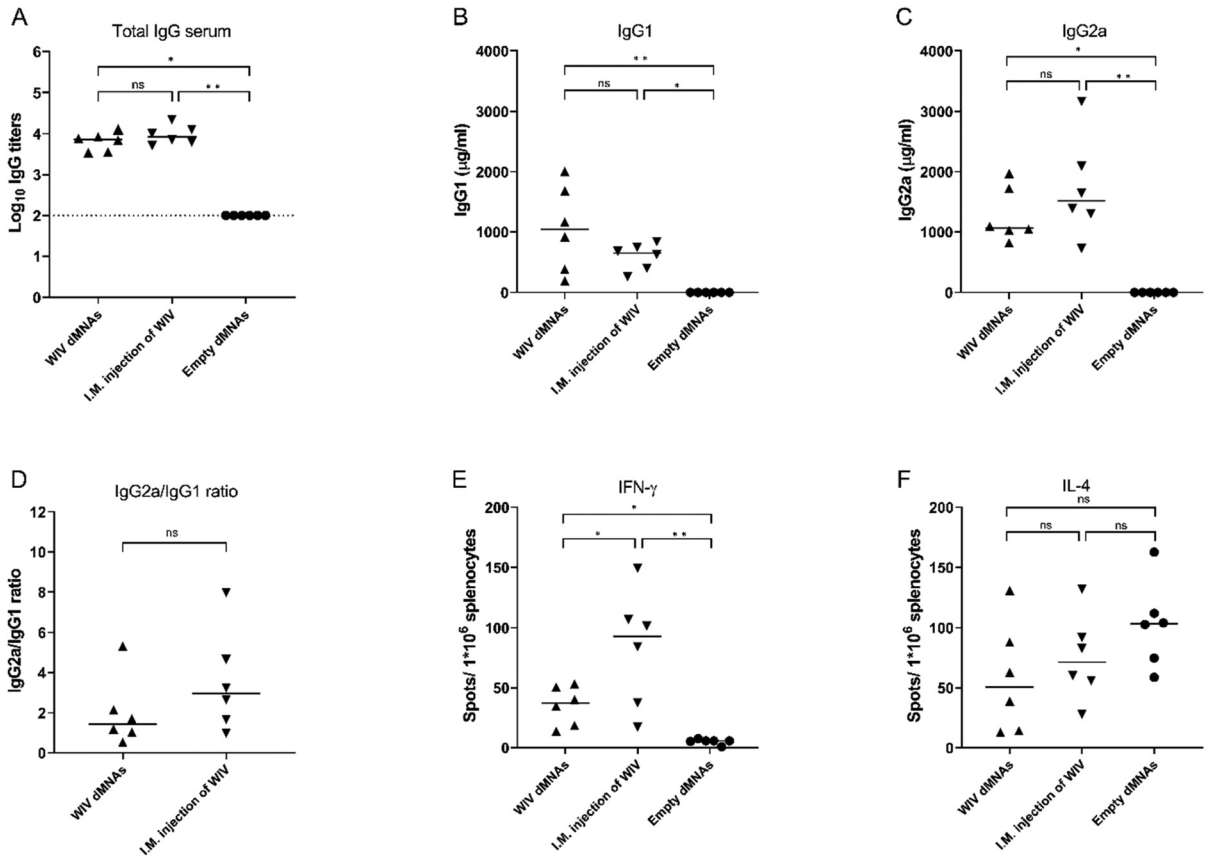

Fig. 6 Humoral and cellular immune responses evoked by immunisation with the dMNA. Mice (n = 6 per experimental group) were immunised with WIV from A/California/07/2009 (H1N1) through administration of freshly prepared dMNAs or by I.M. injection. The control group received empty dMNAs. At day 28 post-immunisation, blood was collected from mice to measure influenza virus-specific IgG (A) titers, as well as IgG1 (B) and IgG2a (C) levels in the serum. The latter two were used to determine the IgG2a to IgG1 ratio per individual mouse (D). Spleens were collected and analysed for IFN-γ producing splenocytes (E) and IL-4 producing splenocytes (F). Statistical comparisons between the different experimental groups were performed using the Kruskal–Wallis test with Dunn's *post hoc* test and the Mann–Whitney test for comparisons between two groups (*$p < 0.05$, ** $p < 0.1$). Individual data and the group median are shown.

First, antigen waste was reduced. Antigen waste is one of the main drawbacks of dMNA fabrication using a centrifuge. In recent studies, only 24% of ovalbumin encapsulated poly (lactic-*co*-glycolic acid) nanoparticles[24] and 1.5% of Qβ-human papillomavirus virus like particles[25] were delivered to the skin from dMNAs. In our previous study, 1 μg of WIV out of 12.5 μg (8%) was delivered into the skin from WIV dMNAs.[12] The main reason was that a substantial fraction of the antigens in dMNAs produced by conventional techniques (*i.e.*, centrifugation and vacuum filling[5]) was incorporated in the backplate of dMNAs which did not release the antigen in the skin. These data indicate that antigen waste is an important challenge to developing cost-effective dMNAs for vaccine delivery. The automatic dispensing system reduced antigen waste by localising the antigen primarily in the microneedle tips, thus lowering antigen waste in the backplate. In contrast to standard vacuum filling, where the whole microneedle mould needs to be in a vacuum chamber (air is removed from the top side of the mould), we developed a method where vacuum is applied from the bottom of the PDMS mould. Thereby, we made use of the nanoporosity of PDMS to remove air from the cavity.[5]

Also, it was hypothesised that the high viscosity of epoxy glue prevented the back-diffusion of drug formulations from the microneedle tip to the backplate. As a result, WIV waste decreased by 94.8% (from 11.5 μg to 0.6 μg) compared to that in the centrifugation method.[12] This result demonstrates the high potential of the automatic dispensing system for the economical production of dMNAs for vaccine delivery especially on an industrial scale. By increasing the number of dispensers and automating the demoulding step, this process can be scaled up.

Second, the dissolution time of the microneedle was reduced. While 1% (w/v) trehalose/pullulan successfully shaped the microneedle structure with the automatic dispensing system, the centrifugation method required 15% (w/v) trehalose/pullulan as a lower concentration failed to build the microneedle structure. Reducing the trehalose/pullulan con-

centration enabled a fast dissolution of microneedles in the skin.[17] In addition, the dispensing method also accelerated the dissolution as it distributed the formulation evenly in the microneedles while the centrifugation method concentrated the formulation in the tips of the microneedle.[24] Hence, the combination of lower concentration and even distribution of the formulation allowed dissolving a larger volume fraction of microneedles in a shorter time period: WIV dMNAs made of 15% (w/v) trehalose/pullulan by the centrifugation method took 15 minutes to dissolve 70% of the microneedle volume,[12] while 10 minutes were enough to dissolve 83% of the microneedle volume for WIV dMNAs made of 1% (w/v) trehalose/pullulan with the automatic dispensing system (section 3.4).[16] The short application time is crucial to facilitate the administration of dMNAs to the population.[26] Lower trehalose/pullulan concentration accelerates the dissolution. In the literature, however, it has been described that a low polymer concentration can decrease the mechanical strength of dMNAs.[17,27] Therefore, the optimisation of the dMNA formulation based on the mechanical strength and the dissolution rate of the microneedles is a necessary step for dMNA fabrication.[26,28] In our previous work, a candidate having a ratio with the lowest portion of pullulan (50% w/w) was chosen among five candidates having different trehalose to pullulan ratios (50 : 50, 40 : 60, 30 : 70, 20 : 80, and 0 : 100) because it dissolved faster than the other four candidates while it still displayed over 90% of penetration efficiency.[12] At the same weight ratio of trehalose/pullulan (50 : 50), the new method of dMNA production using the automatic dispensing system yielded microneedles that effectively pierced the skin without breaking, implying an excellent mechanical strength despite the overall low trehalose/pullulan concentration of only 1% (w/v).

The third advantage of the new production method is the repeatability of dispensing. The automatic dispensing system resulted in less variation in the loading amount of WIV per dMNA than the centrifugation method. The coefficient of variation (ratio of standard deviation to the mean) in antigen load for centrifuged WIV dMNAs was 8.6% [12] while it was only 1.6% for WIV dMNAs produced with the dispensing method (section 3.5). Moreover, for dMNAs produced *via* the centrifugation method, we observed a difference in volume between arrays at the edge of the PDMS mould and arrays in the centre, most probably a result of the centrifugal force. In contrast, the automatic dispensing system produced a constant volume of droplets for all arrays for the desired number of cycles. Therefore, it reduced the difference in the drug loading amount between dMNAs and also between microneedles. In order to increase the repeatability of dMNA fabrication, specialised techniques have been engineered. Droplet-born air blowing[29] and piezoelectric dispensing techniques[15] also use a dispenser and so produce the precise and constant size of droplets. Therefore, these methods can dispense a uniform amount of antigen into each microneedle tip. A micro-injection moulding technique also demonstrated improved repeatability and accurate dosing of dMNAs through a permeation study,[30] and the mould fabricated by the thermal drawing technique increased the reproducibility of the microneedle shape.[31]

Vaccination with WIV dMNAs induced influenza virus-specific antibodies that were at comparable levels to those in I.M. injected mice, but induced lower levels of cellular immune responses than those in I.M. injected mice. Furthermore, the induced humoral and cellular immune responses were skewed towards a Th1 phenotype in both immunisation groups. However, I.M. injected mice had a higher level of Th1-related IgG2a and IFN-γ than the WIV dMNA immunised mice, which is in line with previous influenza vaccination studies comparing I.M. with intradermal immunisation.[32–34] The route of vaccine delivery plays an important role in the induction of Th1-type immunity.[35] To induce high levels of IgG2a and IFN-γ, a high dose of antigen is required to ensure high immune-availability of antigens in the secondary lymphoid organs, whereas low doses of antigen are sufficient to induce Th2-type immunity.[35,36] Hence, the intradermal immunisation with WIV dMNAs may result in lower immune-availability of the influenza antigens in the secondary lymphoid organs of mice compared to the I.M. injection but this remains to be further investigated.

5. Conclusions

In this work, we engineered the WIV dMNA by using an automatic dispensing system that involves plasma treatment of a PDMS mould prior to dispensing and an integrated vacuum system that does not require in-between handling of the microneedle moulds during fabrication. Compared to the centrifugation method, the new method reduced the antigen waste by almost 95%. We found that WIV dMNAs made of 1% (w/v) trehalose/pullulan demonstrated excellent mechanical strength, maintained antigen functionality even after four weeks of storage at RT or 37 °C, and elicited immune responses of similar magnitude to an I.M. injected antigen. We, therefore, consider 1% trehalose/pullulan WIV dMNAs produced by dispensing a promising formulation for the further development of transcutaneous vaccination.

Author contributions

JL: conceptualisation, methodology, validation, formal analysis, investigation, writing – original draft, and review & editing; MB: methodology, investigation, formal analysis, writing – original draft, and review & editing; OAZ: investigation; CO: writing – review & editing and supervision; WLJH: writing – review & editing and supervision; AH: writing – review & editing and supervision; JAB: writing – review & editing, supervision, project administration, and funding acquisition; KvdM: investigation, writing – review & editing, and supervision.

Conflicts of interest

KvdM is a scientific advisor of MyLife Technologies B.V. and co-founder of uPRAX. Other authors declare no conflicts of interest.

Acknowledgements

This work was supported by the Netherlands Organisation for Scientific Research (NWO, TTW15240).

References

1 T. M. Uyeki, High-risk Groups for Influenza Complications, *J. Am. Med. Assoc.*, 2020, **324**(22), 2334. Available from: https://www.ncbi.nlm.nih.gov/pubmed/33136143, [cited 2022 Sep 1].

2 Influenza (Seasonal). [cited 2022 Sep 1]. Available from: https://www.who.int/en/news-room/fact-sheets/detail/influenza-(seasonal).

3 A. S. Monto, F. M. Davenport, J. A. Napier and T. Francis, Effect of vaccination of a school-age population upon the course of an A2-Hong Kong influenza epidemic, *Bull. W. H. O.*, 1969, **41**(3), 537–542. Available from: https://www.ncbi.nlm.nih.gov/pubmed/5309469, [cited 2022 Sep 1].

4 B. Fireman, J. Lee, N. Lewis, O. Bembom, M. van der Laan and R. Baxter, Influenza vaccination and mortality: differentiating vaccine effects from bias, *Am. J. Epidemiol.*, 2009, **170**(5), 650–656. Available from: https://www.ncbi.nlm.nih.gov/pubmed/19625341, [cited 2022 Sep 1].

5 J. H. Park, M. G. Allen and M. R. Prausnitz, Biodegradable polymer microneedles: fabrication, mechanics and transdermal drug delivery, *J. Controlled Release*, 2005, **104**(1), 51–66. Available from: https://pubmed.ncbi.nlm.nih.gov/15866334/, [cited 2023 Jul 3].

6 M. Leone, M. I. Priester, S. Romeijn, M. R. Nejadnik, J. Mönkäre, C. O'Mahony, *et al.*, Hyaluronan-based dissolving microneedles with high antigen content for intradermal vaccination: Formulation, physicochemical characterization and immunogenicity assessment, *Eur. J. Pharm. Biopharm.*, 2019, **134**, 49–59. Available from: https://www.ncbi.nlm.nih.gov/pubmed/30453025, [cited 2023 Jun 9].

7 S. Hirobe, H. Azukizawa, K. Matsuo, Y. Zhai, Y. S. Quan, F. Kamiyama, *et al.*, Development and clinical study of a self-dissolving microneedle patch for transcutaneous immunization device, *Pharm. Res.*, 2013, **30**(10), 2664–2674. Available from: https://www.ncbi.nlm.nih.gov/pubmed/23775442, [cited 2023 Feb 11].

8 J. Arya, S. Henry, H. Kalluri, D. V. McAllister, W. P. Pewin and M. R. Prausnitz, Tolerability, usability and acceptability of dissolving microneedle patch administration in human subjects, *Biomaterials*, 2017, **128**, 1–7. Available from: https://www.ncbi.nlm.nih.gov/pubmed/28285193, [cited 2023 Feb 11].

9 H. S. Gill, D. D. Denson, B. A. Burris and M. R. Prausnitz, Effect of microneedle design on pain in human volunteers, *Clin. J. Pain*, 2008, **24**(7), 585–594. Available from: https://www.ncbi.nlm.nih.gov/pubmed/18716497, [cited 2022 Dec 8].

10 E. V. Vassilieva, H. Kalluri, D. McAllister, M. T. Taherbhai, E. S. Esser, W. P. Pewin, *et al.*, Improved immunogenicity of individual influenza vaccine components delivered with a novel dissolving microneedle patch stable at room temperature, *Drug Delivery Transl. Res.*, 2015, **5**(4), 360–371. Available from: https://link.springer.com/article/10.1007/s13346-015-0228-0, [cited 2022 Aug 29].

11 M. J. Mistilis, J. C. Joyce, E. S. Esser, I. Skountzou, R. W. Compans, A. S. Bommarius, *et al.*, Long-term stability of influenza vaccine in a dissolving microneedle patch, *Drug Delivery Transl. Res.*, 2017, **7**(2), 195–205. Available from: https://www.ncbi.nlm.nih.gov/pubmed/26926241, [cited 2022 Nov 25].

12 Y. Tian, J. Lee, K. van der Maaden, Y. Bhide, J. J. de Vries-Idema, R. Akkerman, *et al.*, Intradermal Administration of Influenza Vaccine with Trehalose and Pullulan-Based Dissolving Microneedle Arrays, *J. Pharm. Sci.*, 2022, **111**(4), 1070–1080. Available from: https://www.ncbi.nlm.nih.gov/pubmed/35122832, [cited 2022 Mar 31].

13 J. F. Liao, J. C. Lee, C. K. Lin, K. C. Wei, P. Y. Chen and H. W. Yang, Self-Assembly DNA Polyplex Vaccine inside Dissolving Microneedles for High-Potency Intradermal Vaccination, *Theranostics*, 2017, **7**(10), 2593–2605. Available from: https://www.ncbi.nlm.nih.gov/pubmed/28819449, [cited 2022 Aug 29].

14 M. G. McGrath, S. Vucen, A. Vrdoljak, A. Kelly, C. O'Mahony, A. M. Crean, *et al.*, Production of dissolvable microneedles using an atomised spray process: Effect of microneedle composition on skin penetration, *Eur. J. Pharm. Biopharm.*, 2014, **86**(2), 200–211.

15 E. A. Allen, C. O'mahony, M. Cronin, T. O'mahony, A. C. Moore and A. M. Crean, Dissolvable microneedle fabrication using piezoelectric dispensing technology, *Int. J. Pharm.*, 2015, **500**(1–2), 1–10. Available from: https://www.ncbi.nlm.nih.gov/pubmed/26721722, [cited 2022 Sep 5].

16 A. Vrdoljak, E. A. Allen, F. Ferrara, N. J. Temperton, A. M. Crean and A. C. Moore, Induction of broad immunity by thermostabilised vaccines incorporated in dissolvable microneedles using novel fabrication methods, *J. Controlled Release*, 2016, **225**, 192–204.

17 J. Lee, K. van der Maaden, G. Gooris, C. O'Mahony, W. Jiskoot and J. Bouwstra, Engineering of an automated nano-droplet dispensing system for fabrication of antigen-loaded dissolving microneedle arrays, *Int. J. Pharm.*, 2021, **600**, 120473. Available from: https://www.ncbi.nlm.nih.gov/pubmed/33737094, [cited 2021 Mar 29].

18 J. Tomar, H. P. Patil, G. Bracho, W. F. Tonnis, H. W. Frijlink, N. Petrovsky, *et al.*, Advax augments B and T cell responses upon influenza vaccination via the respiratory tract and enables complete protection of mice against lethal influenza virus challenge, *J. Controlled Release*, 2018,

288(June), 199–211. Available from: https://www.ncbi.nlm.nih.gov/pubmed/30218687.

19 S. A. L. Audouy, G. van der Schaaf, W. L. J. Hinrichs, H. W. Frijlink, J. Wilschut and A. Huckriede, Development of a dried influenza whole inactivated virus vaccine for pulmonary immunization, *Vaccine*, 2011, **29**(26), 4345–4352. Available from: https://www.ncbi.nlm.nih.gov/pubmed/21514345.

20 M. Leone, M. I. Priester, S. Romeijn, M. R. Nejadnik, J. Mönkäre, C. O'mahony, *et al.*, Hyaluronan-based dissolving microneedles with high antigen content for intradermal vaccination: formulation, physicochemical characterization and immunogenicity assessment, *Eur. J. Pharm. Biopharm.*, 2018, **134**, 49–59.

21 H. Liu, H. P. Patil, J. de Vries-Idema, J. Wilschut and A. Huckriede, Enhancement of the Immunogenicity and Protective Efficacy of a Mucosal Influenza Subunit Vaccine by the Saponin Adjuvant GPI-0100, Ambrose Z, editor, *PLoS One*, 2012, 7(12), e52135.

22 S. P. Gadani, J. C. Cronk, G. T. Norris and J. Kipnis, IL-4 in the brain: a cytokine to remember, *J. Immunol.*, 2012, **189**(9), 4213–4219. Available from: https://pubmed.ncbi.nlm.nih.gov/23087426/, [cited 2023 Jul 17].

23 C. M. Snapper and W. E. Paul, Interferon-gamma and B cell stimulatory factor-1 reciprocally regulate Ig isotype production, *Science*, 1987, **236**(4804), 944–947.

24 J. Mönkäre, M. Pontier, E. E. M. van Kampen, G. Du, M. Leone, S. Romeijn, *et al.*, Development of PLGA nanoparticle loaded dissolving microneedles and comparison with hollow microneedles in intradermal vaccine delivery, *Eur. J. Pharm. Biopharm.*, 2018, **129**, 111–121.

25 S. Ray, D. M. Wirth, O. A. Ortega-Rivera, N. F. Steinmetz and J. K. Pokorski, Dissolving Microneedle Delivery of a Prophylactic HPV Vaccine, *Biomacromolecules*, 2022, **23**(3), 903–912, DOI: 10.1021/acs.biomac.1c01345, [cited 2023 Jan 14].

26 S. Amodwala, P. Kumar and H. P. Thakkar, Statistically optimized fast dissolving microneedle transdermal patch of meloxicam: A patient friendly approach to manage arthritis, *Eur. J. Pharm. Sci.*, 2017, **104**, 114–123.

27 M. Kim, H. Yang, H. Kim, H. Jung and H. Jung, Novel cosmetic patches for wrinkle improvement: retinyl retinoate- and ascorbic acid-loaded dissolving microneedles, *Int. J. Cosmet. Sci.*, 2014, **36**(3), 207–212. Available from: https://www.ncbi.nlm.nih.gov/pubmed/24910870, [cited 2023 Jan 14].

28 Z. Cheng, H. Lin, Z. Wang, X. Yang, M. Zhang, X. Liu, *et al.*, Preparation and characterization of dissolving hyaluronic acid composite microneedles loaded micelles for delivery of curcumin, *Drug Delivery Transl. Res.*, 2020, **10**(5), 1520–1530. Available from: https://www.ncbi.nlm.nih.gov/pubmed/32100266, [cited 2022 Oct 6].

29 J. D. Kim, M. Kim, H. Yang, K. Lee and H. Jung, Droplet-born air blowing: novel dissolving microneedle fabrication, *J. Controlled Release*, 2013, **170**(3), 430–436. Available from: https://www.ncbi.nlm.nih.gov/pubmed/23742882, [cited 2022 Sep 1].

30 C. Uppuluri, A. S. Shaik, T. Han, A. Nayak, K. J. Nair, B. R. Whiteside, *et al.*, Effect of Microneedle Type on Transdermal Permeation of Rizatriptan, *AAPS PharmSciTech*, 2017, **18**(5), 1495–1506. Available from: https://www.ncbi.nlm.nih.gov/pubmed/28078629, [cited 2022 Sep 6].

31 J. Y. Lee, S. H. Park, I. H. Seo, K. J. Lee and W. H. Ryu, Rapid and repeatable fabrication of high A/R silk fibroin microneedles using thermally-drawn micromolds, *Eur. J. Pharm. Biopharm.*, 2015, **94**, 11–19.

32 Y. C. Kim, F. S. Quan, D. G. Yoo, R. W. Compans, S. M. Kang and M. R. Prausnitz, Enhanced memory responses to H1N1 influenza vaccination in the skin using vaccine coated-microneedles, *J. Infect. Dis.*, 2010, **201**(2), 190. Available from: https://www.ncbi.nlm.nih.gov/pubmed/20017632, [cited 2022 Sep 12].

33 A. Lysén, R. Braathen, A. Gudjonsson, D. Y. Tesfaye, B. Bogen and E. Fossum, Dendritic cell targeted Ccl3- and Xcl1-fusion DNA vaccines differ in induced immune responses and optimal delivery site, *Sci. Rep.*, 2019, **9**(1), 1–11. Available from: https://www.ncbi.nlm.nih.gov/pubmed/30755656, [cited 2022 Sep 12].

34 F. S. Quan, Y. C. Kim, A. Vunnava, D. G. Yoo, J. M. Song, M. R. Prausnitz, *et al.*, Intradermal Vaccination with Influenza Virus-Like Particles by Using Microneedles Induces Protection Superior to That with Intramuscular Immunization, *J. Virol.*, 2010, **84**(15), 7760w. Available from: https://www.ncbi.nlm.nih.gov/pubmed/20484519, [cited 2022 Sep 12].

35 D. Mohanan, B. Slütter, M. Henriksen-Lacey, W. Jiskoot, J. A. Bouwstra, Y. Perrie, *et al.* Administration routes affect the quality of immune responses: A cross-sectional evaluation of particulate antigen-delivery systems, *J. Controlled Release*, 2010, **147**(3), 342–349. Available from: https://www.ncbi.nlm.nih.gov/pubmed/20727926, [cited 2022 Sep 12].

36 N. A. Hosken, K. Shibuya, A. W. Heath, K. M. Murphy and A. O'Garra, The effect of antigen dose on CD4+ T helper cell phenotype development in a T cell receptor-alpha beta-transgenic model, *J. Exp. Med.*, 1995, **182**(5), 1579–1584. Available from: https://www.ncbi.nlm.nih.gov/pubmed/7595228, [cited 2022 Sep 12].

